

# Supporting Information

## Effect of Thermal Annealing in Ammonia on the Properties of InGaN Nanowires with Different Indium Concentration

*Christopher Hahn, Amy A. Cordones<sup>¶</sup>, Sean C. Andrews, Hanwei Gao, Anthony Fu, Stephen R. Leone<sup>¶,§</sup> and Peidong Yang\**

Department of Chemistry, University of California, Berkeley, California 94720

Materials Sciences Division, Lawrence Berkeley National Laboratory, 1 Cyclotron Road,  
Berkeley, California 94720

<sup>¶</sup>Chemical Sciences Division, Lawrence Berkeley National Laboratory, 1 Cyclotron  
Road, Berkeley, California 94720

<sup>§</sup>Department of Physics, University of California, Berkeley, California 94720

\*Address correspondence to [p\\_yang@berkeley.edu](mailto:p_yang@berkeley.edu)

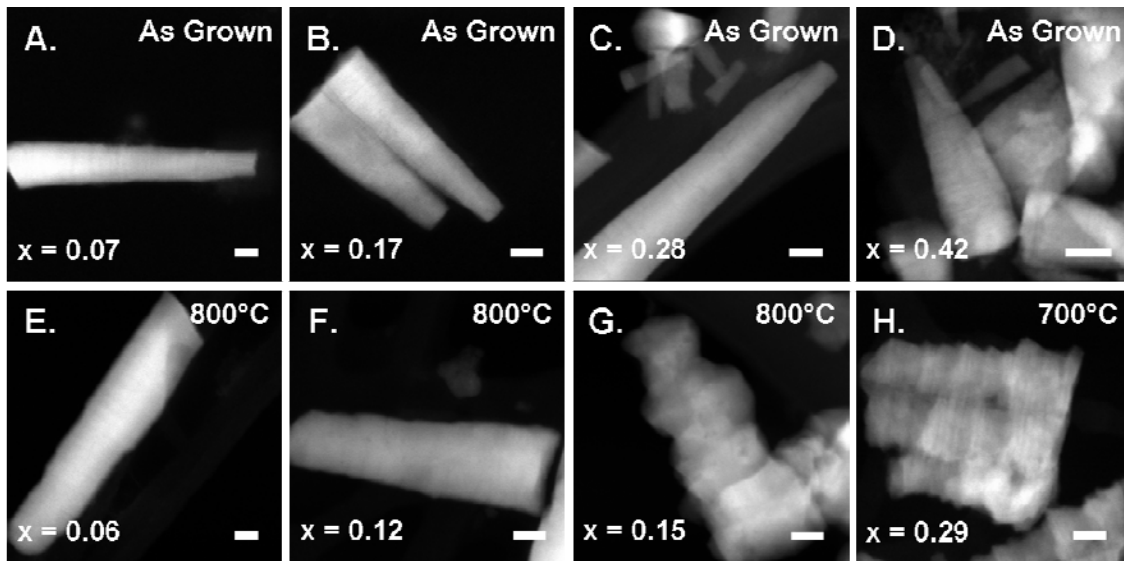


**Figure S11.** HAADF STEM images of as grown and annealed  $\text{In}_x\text{Ga}_{1-x}\text{N}$  nanowires. HAADF STEM images of (A-D) as grown and (E-H) annealed nanowires show the instability of  $\text{In}_x\text{Ga}_{1-x}\text{N}$  nanowires with from increasing the indium composition. Significant surface etching was observed for samples (C,G)  $x = 0.28$  and (D,H)  $x = 0.42$  after annealing. Scale bar = 20 nm.

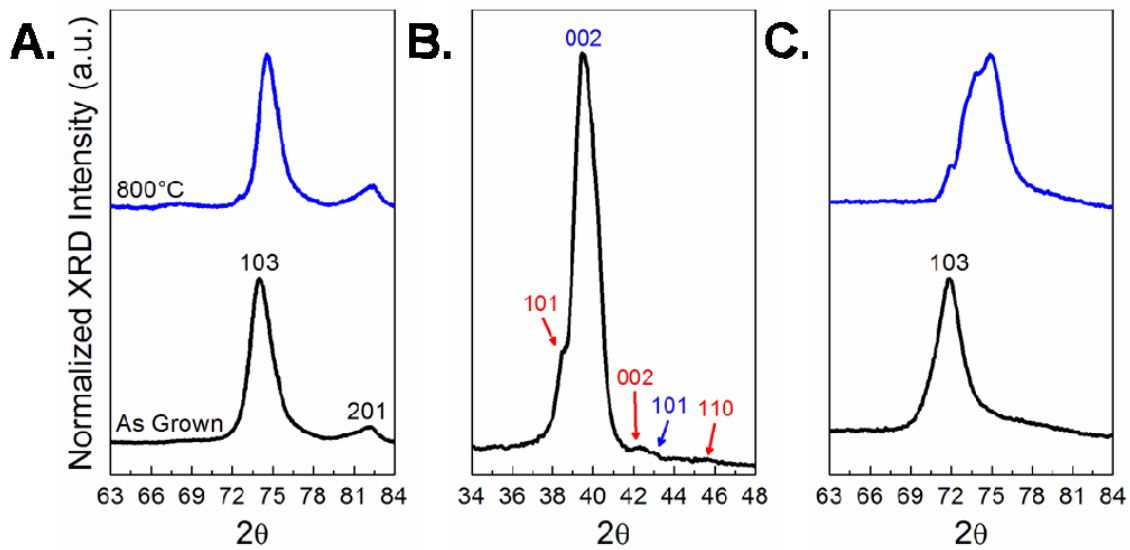


**Figure SI2.** XRD spectra of as grown and annealed  $\text{In}_x\text{Ga}_{1-x}\text{N}$  nanowires. (A) High angle wurtzite 103 and 201 diffraction peaks for sample  $x = 0.17$  show no peak splitting after annealing, indicating that lower indium composition nanowires are phase stable. (B) The XRD spectrum for sample  $x = 0.42$  reveals  $\text{In}_x\text{Ga}_{1-x}\text{N}$  wurtzite (blue) and In tetragonal (red) peaks, showing that nanowires decompose into In metal during the annealing process. (C) The high angle wurtzite 103 peak for sample  $x = 0.42$  splits into multiple peaks after annealing at  $800^\circ\text{C}$ , indicating that higher indium composition  $\text{In}_x\text{Ga}_{1-x}\text{N}$  nanowires are metastable and phase separate at high temperatures.

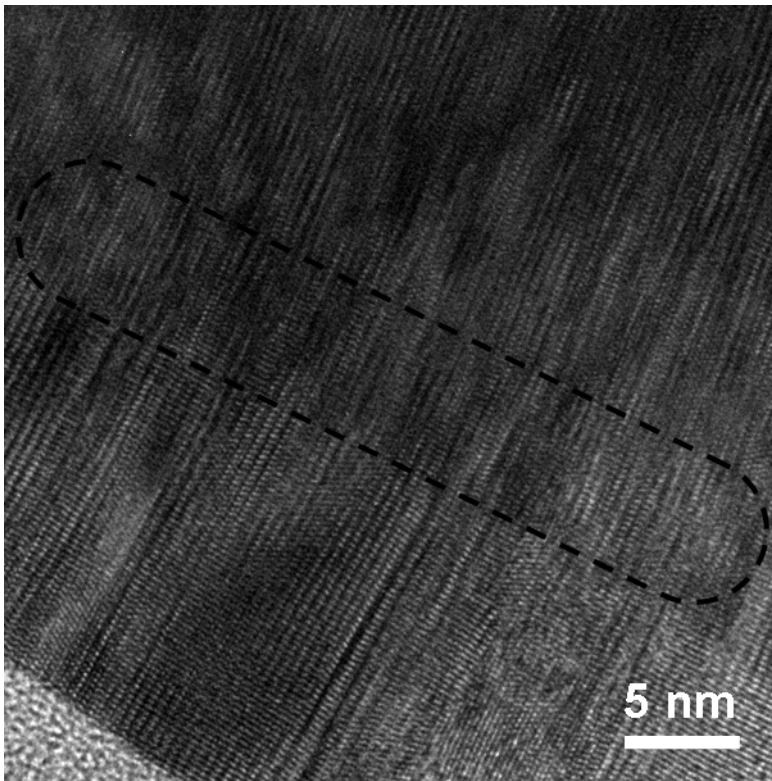


**Figure SI3.** HRTEM image of sintered  $\text{InGaN}$  nanowires. The HRTEM image shows a clear shift in lattice orientation from the bottom nanowire to the top nanowire, indicating that as grown  $\text{InGaN}$  nanowires are likely tilted/twisted in orientation from mosaic

growth. As a result, an increase in dislocation density can be seen at the interface of sintered InGaN nanowires (dashed area).

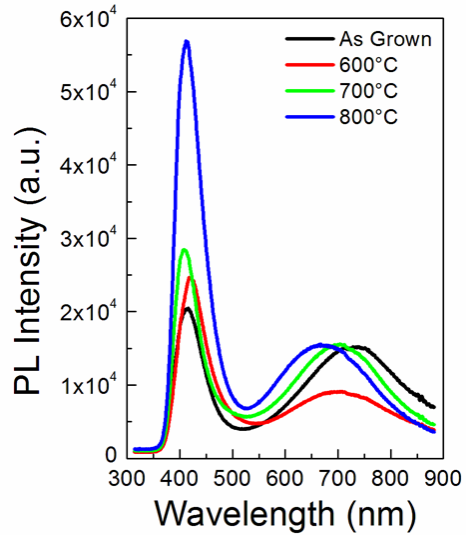


**Figure SI4.** PL spectra of as grown and annealed  $\text{In}_x\text{Ga}_{1-x}\text{N}$  nanowires. PL spectra for sample  $x = 0.07$  show that the intensity of band-edge PL increases with annealing temperature.

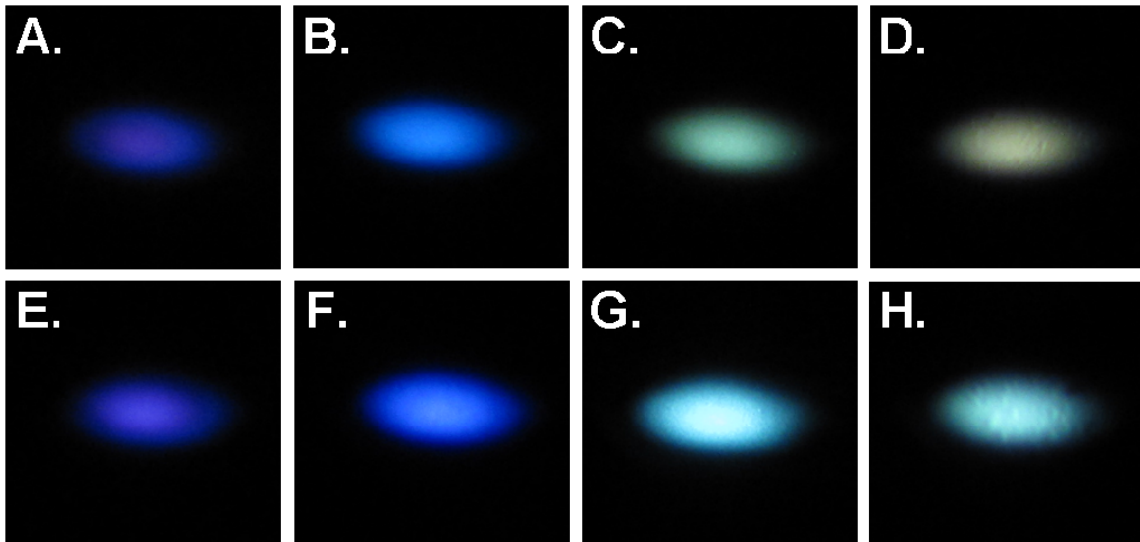


**Figure SI5.** Color PL images of as grown and annealed  $\text{In}_x\text{Ga}_{1-x}\text{N}$  nanowires. Color PL images of as grown samples (A)  $x = 0.07$ , (B)  $x = 0.17$ , (C)  $x = 0.28$ , and (D)  $x = 0.42$  demonstrate the ability to tune the emission wavelength with indium composition. (E-H) The corresponding annealed nanowire arrays increase in intensity from an improvement in QE. (G,H) The PL of higher indium composition arrays changes in color from indium etching.

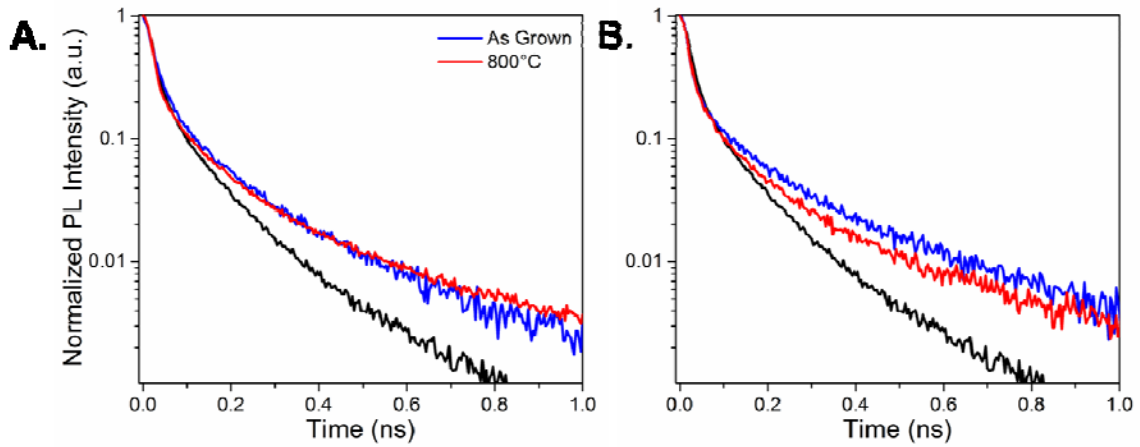


**Figure SI6.** Time-resolved PL spectra of as grown and annealed  $\text{In}_x\text{Ga}_{1-x}\text{N}$  nanowires. Time-resolved PL spectra of as grown and annealed samples (A)  $x = 0.28$  and (B)  $x = 0.42$  show fast initial decay of the PL intensity. The majority of the signal is limited by the instrument response function (shown in black).